Science Immunology

immunology.sciencemag.org/cgi/content/full/1/6/eaai8593/DC1

Supplementary Materials for

The TCF1-Bcl6 axis counteracts type I interferon to repress exhaustion and maintain T cell stemness

Tuoqi Wu,* Yun Ji, E. Ashley Moseman, Haifeng C. Xu, Monica Manglani, Martha Kirby, Stacie M. Anderson, Robin Handon, Elizabeth Kenyon, Abdel Elkahloun, Weiwei Wu, Philipp A. Lang, Luca Gattinoni, Dorian B. McGavern, Pamela L. Schwartzberg*

*Corresponding author. Email: pams@nhgri.nih.gov (P.L.S.); tuoqi.wu@nih.gov (T.W.)

Published 9 December 2016, *Sci. Immunol.* **1**, eaai8593 (2016)
DOI: 10.1126/sciimmunol.aai8593

The PDF file includes:

Materials and Methods
Fig. S1. T_{FH}-like CD8 T cells generated after chronic LCMV clone 13 infection.
Fig. S2. $TCF1^{high}Tim3^{low}$ virus-specific CD8 T cells are less exhausted and persist better during chronic viral infection.
Fig. S3. TCF1 is required for the differentiation of $Tim3^{low}$ virus-specific CD8 T cells and long-term persistence of T cell responses.
Fig. S4. TCF1 is intrinsically required for the development of $Tim3^{low}$ virus-specific CD8 T cells and sustained T cell responses.
Fig. S5. Numbers of TCF1-overexpressing and control P14 cells on day 8 after infection.
Fig. S6. GSEA of microarray data from TCF1 KO and overexpression experiments.
Fig. S7. Type I IFN blockade enhanced the generation of $TCF1^{high}Tim3^{low}$ virus-specific CD8 T cells.
Legends for tables S1 to S4

Other Supplementary Material for this manuscript includes the following:
(available at immunology.sciencemag.org/cgi/content/full/1/6/eaai8593/DC1)

Table S1 (Microsoft Excel format). Differentially expressed genes between $Tim3^{-}Blimp1^{-}$ and $Tim3^{+}Blimp1^{+}$ CD8 T cells.
Table S2 (Microsoft Excel format). Differentially expressed genes between Tcf7 KO and WT CD8 T cells.
Table S3 (Microsoft Excel format). Differentially expressed genes between TCF1-overexpressing and MIG P14 cells.
Table S4 (Microsoft Excel format). Raw data and statistical analyses.

Materials and Methods

Mice

Tcf7$^{loxP/loxP}$; CD4-Cre (cKO) mice have been described previously (*21*). Blimp1-YFP reporter mice (*47*), C57Bl6, and WT CD45.1 (B6.SJL-Ptprca Pepcb/BoyJ) were obtained from the Jackson Laboratory. P14 transgenic mice express a TCR clone that recognizes GP33 eptitope on LCMV (*31*). *Ifnar1* KO P14 mice were described previously (*38*). Mice were maintained on a C57Bl6 background under specific pathogen-free conditions prior to infection with LCMV Clone 13. All animal husbandry and experiments were approved by the National Human Genome Research Institute, the National Institute of Neurological Disorders and Stroke, or the National Cancer Institute Animal Use and Care Committees, or by the authorization of the LANUV in accordance with German laws for animal protection.

Viral infection, adoptive transfers and mixed bone marrow chimeras and tumor implantation

Mice were intravenously (i.v.) injected with 2×10^6 plaque-forming unit (PFU) LCMV clone 13. Viral titers were determined by plaque assay using Vero cells as described (*48*). For the adoptive transfer experiments, Tim3^{low}PD1^{+}CD44^{high} and Tim3^{high}PD1^{+}CD44^{high} CD8 T cells were FACS sorted from C57Bl6 mice 7 days after LCMV clone 13 infection. 10^6 donor cells of each population were transferred separately into naïve to study recall response or into infection-matched CD45.1 mice for lineage tracing. Naïve mice that had received donor cells were infected with LCMV clone 13. Mixed bone marrow chimeras were generated by injecting lethally irradiated WT CD45.1 mice with mixed bone marrow from a WT CD45.1 donor, and a CD45.2 donor that was either *Tcf7* WT or cKO. Chimeras were used for experiments after at least two months from the date of reconstitution. For tumor implantation, $0.5\sim1\times10^6$ MCA205 sarcoma cells were injected subcutaneously in the flank of C57Bl6 mice.

Phenotypic analysis of human melanoma TIL.

All human samples were obtained in the course of a US National Cancer Institute Institutional Review Board–approved clinical trials (NCT01236573 and NCT01319565). Tumor samples were thawed in the presence of 3 U/ml DNAse (Genentech Inc.), and rested overnight in a 1:1 mix of RPMI-1640 with l-glutamine (Lonza) and AIM-V (Gibco) supplemented with 100 U/ml penicillin, 100 μg/ml streptomycin, 12.5 mM HEPES, and 5% AB human serum (Valley Biomedical). This overnight resting period was carefully assessed and necessary for the recovery of expression cell surface receptors affected by cryopreservation or subject to cleavage during the enzymatic digest. Cells were harvested, counted, blocked with Fc block and stained with the specified antibodies.

Type I interferon blockade and NK-cell depletion

For IFNAR1 blockade, mice were intraperitoneally injected with one mg anti-IFNAR1 (MAR1-5A3) one day prior to infection. For NK-cell depletion, mice were injected with 2 doses of 300 ug anti-NK1.1 (PK136) one day before and after infection.

Retroviral transduction

TCF1 (Uniprot, Q00417-2) and Bcl6 over-expression constructs on an MSCV-IRES-GFP backbone (MIG) have been described previously (*21*). IFNAR1 shRNA (5'-GAATGAGGTTGATCCGTTTAT-3') was cloned into pMKO.1-GFP backbone as described previously (*21*). Activated P14 CD8 T cells were spin-infected with retroviruses for 90 minutes, cultured overnight, and FACS sorted for GFP^+ transduced CD8 T cells. Purified cells were injected into C57Bl6 recipients, which were subsequently infected with LCMV clone 13.

Antibodies, dyes, flow cytometry and cell sorting

Anti-mouse CD4 (RM4-5), anti- mouse CD8a (53-6.7), anti-human CD8a (RPA-T8), anti- mouse LAG3 (C9B7W), anti- mouse CD45.1 (A20), and anti- mouse CD45.2 (104) were from eBioscience; anti-mouse 2B4 and anti-Bcl6 (K112-91) were from BD Biosciences; anti- mouse PD1 (RMP1-30), anti-mouse SLAM (TC15-12F12.2) and anti-human PD1 (EH12.2h7) were from Biolegend; anti-mouse Tim3 (215008) and anti-human Tim3 (344823) were from R&D. IA^bGP66-77 tetramer staining has been described elsewhere (*49*). All tetramers were obtained from NIAID Tetramer Core Facility. TCF1 staining has been described in our previous study (*21*). All flow cytometry analyses were performed on BD™ LSR II. Data were processed with FlowJo 9.8. FACS sorting was performed on BD FACSAria™ II.

RNA purification and microarray analysis

Tetramer$^+$ $Tim3^{low}Blimp1^{low}$ and $Tim3^{high}Blimp1^{high}$ CD8 T cells for the experiment described in Fig. 1C, tetramer$^+$ *Tcf7* cKO and WT CD8 T cells for the experiment described in Fig. 6A, or control and TCF1 over-expressing P14 cells for the experiment described in Fig. 6C were FACS sorted to purities >98%. Total RNA was extracted with miRNeasy Mini kit (Qiagen) from 3 independent experiments for each sample and control, and genomic DNA was eliminated with RNase-Free DNase Set (Qiagen). RNA quality and quantity were examined by Bioanalyzer (Agilent) and NanoDrop (Thermo Scientific), respectively. Microarray experiments were performed using RNA from 3 independent biological replicates on GeneChip® Mouse Gene 2.0 ST Arrays (Affymetrix). Microarray data were analyzed with Partek Genomic Suite (Partek Inc.). Microarray data have been deposited in GEO under accession number GSE85367.

Chromatin immunoprecipitation (ChIP)

$Tim3^{low}PD1^{+}CD44^{high}$ and $Tim3^{high}PD1^{+}CD44^{high}$ CD8 T cells were FACS sorted from C57Bl6 mice 7 days after LCMV clone 13 infection. ChIP experiments were performed on ~5×10^{6} cells according to the manufacturer's instructions with ChIP assay kit (Millipore). Anti-TCF1 (SantaCruz, sc-13025) was used. The enrichment of target loci by ChIP was determined by QRT-PCR. Primers used in QRT-PCR to amplify *Bcl6* promoter were: 5'- gggtctggggctaattcttc -3' (Forward) and 5'- tagctggaaggagctgtggt -3' (Reverse); third intron of *Prdm1* were: 5'- gtgtggcttcatcaaagcag-3' (Forward) and 5'- gaagtttgcgcgtcagagta-3' (Reverse); -7 kb from *Havcr2* TSS were: 5'- cctgaagctcaccaaacctc-3' (Forward) and 5'- tggcagtctttgcttccttt-3' (Reverse); *Cish* promoter were: 5'- ctttctcggtccaaagcact-3' (Forward) and 5'- gaacagcttggaaggacgag-3' (Reverse).

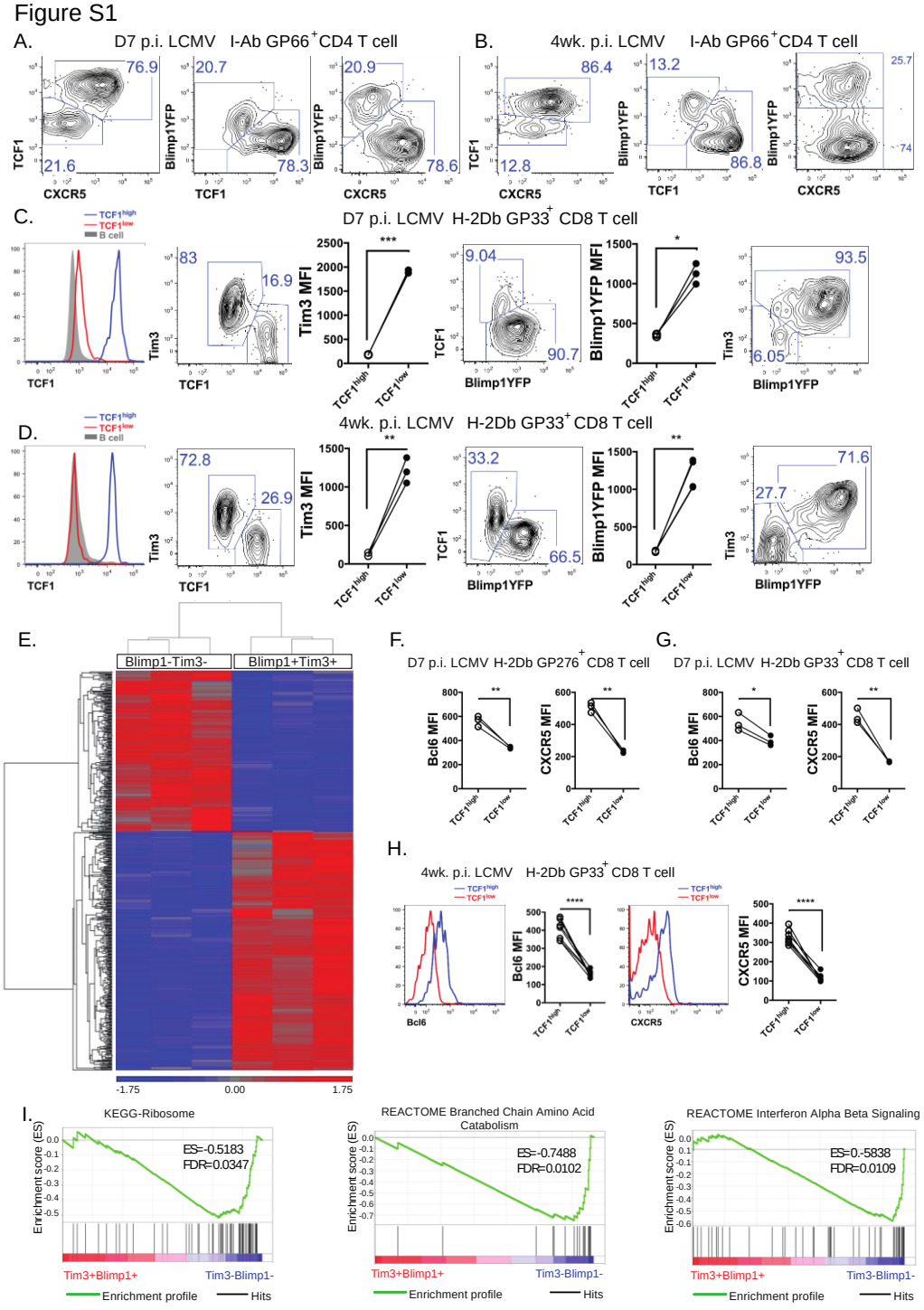

Fig. S1. TFH-like CD8 T cells generated after chronic LCMV clone 13 infection. (A-D) C57Bl6 or Blimp1-YFP reporter mice were infected by LCMV clone 13. (A, B) Expression of TCF1, CXCR5, and Blimp1 in I-Ab GP66 tetramer+ CD4 T cells in the spleen were analyzed on day 7 (A) and 4 wk (B) p.i.

(C, D) Expression of TCF1, Tim3, and Blimp1 in H-2Db GP33 tetramer^{+} CD8 T cells in the spleen were analyzed on day 7 (C) and 4 wk (D) p.i. (E) Hierarchical clustering of microarray data in Table S1 to demonstrate the triplicate concordance of differentially expressed genes. (F-H) Expression of Bcl6 and CXCR5 in H-2Db GP33 tetramer^{+} (G, H) or H-2Db GP276 tetramer^{+} (F) CD8 T cells in the spleen were analyzed on day 7 (F, G) and 4 wk (H) p.i. (I) GSEA of the microarray data in Fig. 1C to compare the enrichment of gene signatures of Ribosome (left), branched-chain amino acid catabolism (middle), and type I interferon signaling (right) between Tim3^{low}Blimp1^{low} and Tim3^{high}Blimp1^{high} virus-specific CD8 T cells. Data in (A-D, F-H) are representative of at least two independent experiments with $n \geq 3$. Statistical significance in (A-D, F-H) was determined by paired t tests.

*$p<0.05$,**$p<0.01$,***$p<0.001$,****$p<0.0001$ for all figures.

Figure S2

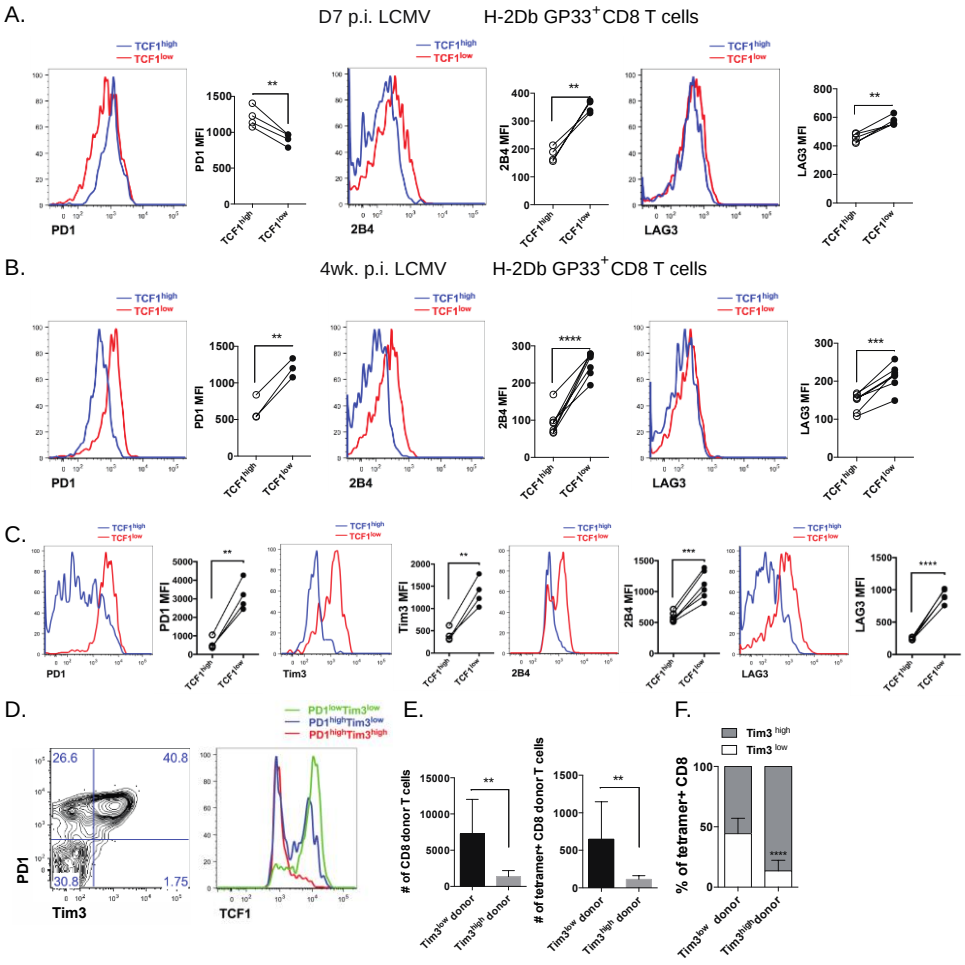

Fig. S2. TCF1^{high}Tim3^{low} virus-specific CD8 T cells are less exhausted and persist better during chronic viral infection. (A, B) C57Bl6 mice were infected with LCMV clone 13. PD1, 2B4, and LAG3 expression on TCF1^{high} (blue) and TCF1^{low} (red) H-2Db GP33 tetramer^{+} CD8 T cells in the spleen analyzed on day 7 p.i. (A) and 4 weeks p.i. (B). (C) Expression of PD1, Tim3, 2B4, and LAG3 on TCF1^{high} (blue) and TCF1^{low} (red) CD8 T cells infiltrating MCA205 tumors. (D) TCF1 expression in PD1^{high}Tim3^{high}, PD1^{high}Tim3^{low}, and PD1^{low}Tim3^{low} subsets of CD8 TILs from MCA205 tumors. (E, F) Tim3^{low}PD1^{+}CD44^{high} and Tim3^{high}PD1^{+}CD44^{high} CD8 T cells were sorted from C57Bl6 mice on day 7 p.i., and transferred separately into infection-matched CD45.1 mice. (E) The numbers of donor CD8 T

cells and tetramer^{+} donor CD8 T cells in the spleen from each group were determined on day 7 post-transfer. (F) The frequencies of Tim3^{low} (white) and Tim3^{high} (grey) cells within tetramer^{+} progeny from Tim3^{low} or Tim3^{high} donors were determined. Data are representative of at least two independent experiments with $n \geq 3$. Statistical significance was determined by paired t tests (A-C) and unpaired t tests (E, F).

Figure S3

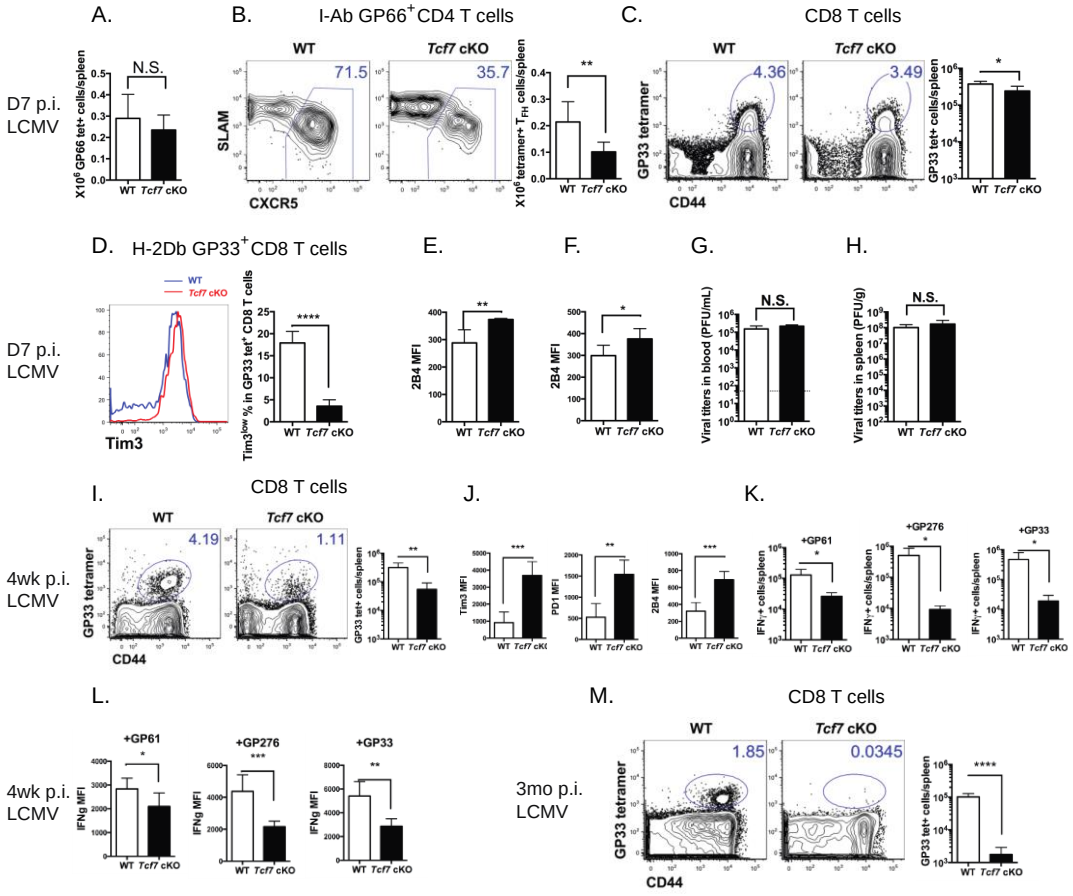

Fig. S3. TCF1 is required for the differentiation of Tim3^{low} virus-specific CD8 T cells and long-term persistence of T cell responses. *Tcf7*$^{loxP/loxP}$CD4-Cre (*Tcf7* cKO) and littermate control (WT) mice were infected with LCMV clone 13. (A) Numbers of WT and cKO I-Ab GP66 tetramer^{+} CD4 T cells on day 7 p.i. (B) Representative FACS plots of CXCR5 and SLAM expression in I-Ab GP66 tetramer^{+} CD4 T cells and numbers of I-Ab GP66 tetramer^{+} T_{FH} (CXCR5^{+}SLAM^{low}) cells in the spleen from WT and cKO mice on day 7 p.i. (C) Representative FACS plots of H-2Db GP33 tetramer staining and numbers of H-2Db GP33 tetramer^{+} CD8 T cells in the spleen from WT and cKO mice on day 7 p.i. (D) Representative histograms of Tim3 expression in H-2Db GP33 tetramer^{+} WT (blue) and cKO (red) CD8 T cells and frequencies of Tim3^{low} cells within H-2Db GP33 tetramer^{+} WT and cKO CD8 T cells

on day 7 p.i. (E, F) Expression of 2B4 on H-2Db GP276 tetramer$^+$ (E) and H-2Db GP33 tetramer$^+$ (F) CD8 T cells in the spleen from WT and cKO mice on day 7 p.i. Blood (G) and spleen (H) viral titers from WT and cKO mice on day 7 p.i. (I) Representative FACS plots of H-2Db GP33 tetramer staining and numbers of WT and cKO H-2Db GP33 tetramer$^+$ CD8 T cells in the spleen from mice 4 weeks p.i. (J) Expression of Tim3, PD1, and 2B4 on H-2Db GP33 tetramer$^+$ CD8 T cells in the spleen from WT and cKO mice 4 weeks p.i. (K, L) Numbers of IFNγ$^+$ CD4 or CD8 T cells in the spleen 4 weeks p.i. (K) and IFNγ expression levels within IFNγ$^+$ CD4 or CD8 T cells (L) after re-stimulation with GP61, GP276, or GP33 peptide. (M) Representative FACS plots of H-2Db GP33 tetramer staining and numbers of H-2Db GP33 tetramer$^+$ CD8 T cells in the spleen from WT and cKO mice 3 months p.i. Data are representative of at least two independent experiments with n≥3. Statistical significance was determined by unpaired t tests.

Figure S4

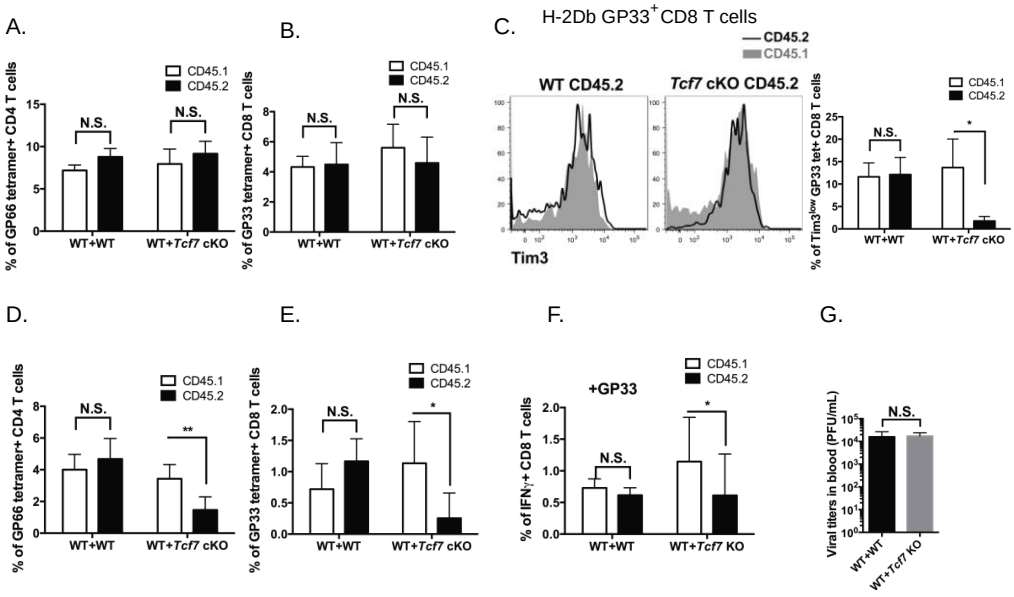

Fig. S4. TCF1 is intrinsically required for the development of Tim3^{low} virus-specific CD8 T cells and sustained T cell responses. Mixed bone marrow chimeras were generated and infected as described in Fig. 4. (A, B) On day 7 p.i., frequencies of I-Ab GP66 tetramer^{+} (A) and frequencies of H-2Db GP33 tetramer^{+} (B) cells within CD45.1 (white) and CD45.2 (filled) CD4 or CD8 T cell compartments in the spleen from chimeras were determined. (C) Tim3 expression on H-2Db GP33 tetramer^{+} WT CD45.1 (shaded) as well as WT and *Tcf7* cKO CD45.2 (solid line) CD8 T cells and frequencies of Tim3^{low} cells within H-2Db GP33 tetramer^{+} WT CD45.1 (white) as well as WT and *Tcf7* cKO CD45.2 (filled) CD8 T cells in the spleen from chimeras on day 7 p.i. (D) Frequencies of I-Ab GP66 tetramer^{+} cells within CD45.1 (white) and CD45.2 (filled) CD4 compartments in the spleen from chimeras 4 weeks p.i. (E) Frequencies of H-2Db GP33 tetramer^{+} cells within WT CD45.1 (white) as well as WT and *Tcf7* cKO CD45.2 (filled) CD8 T cells in the spleen from chimeras 4 weeks p.i. (F) Frequencies of IFNγ^{+} cells within WT CD45.1 (white) as well as WT and *Tcf7* cKO CD45.2 (filled) CD8 T cells in the spleen from chimeras 4 weeks p.i after re-stimulation with GP33 peptide for 5 hr. (G)

Blood viral titers from chimeras 4 week p.i. Data are representative of at least two independent experiments with n≥4. Statistical significance was determined by paired t tests (A-F) and unpaired t tests (G).

Figure S5

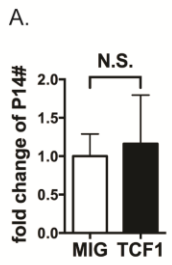

Fig. S5. Numbers of TCF1-overexpressing and control P14 cells on day 8 after infection. P14 cells were transduced with control (MIG) or TCF1 over-expression (TCF1) construct and transferred into C57Bl6 mice that were subsequently infected with LCMV clone 13. Numbers of control and TCF1 over-expressing P14 cells in the spleen were determined on day 8 p.i.

Figure S6

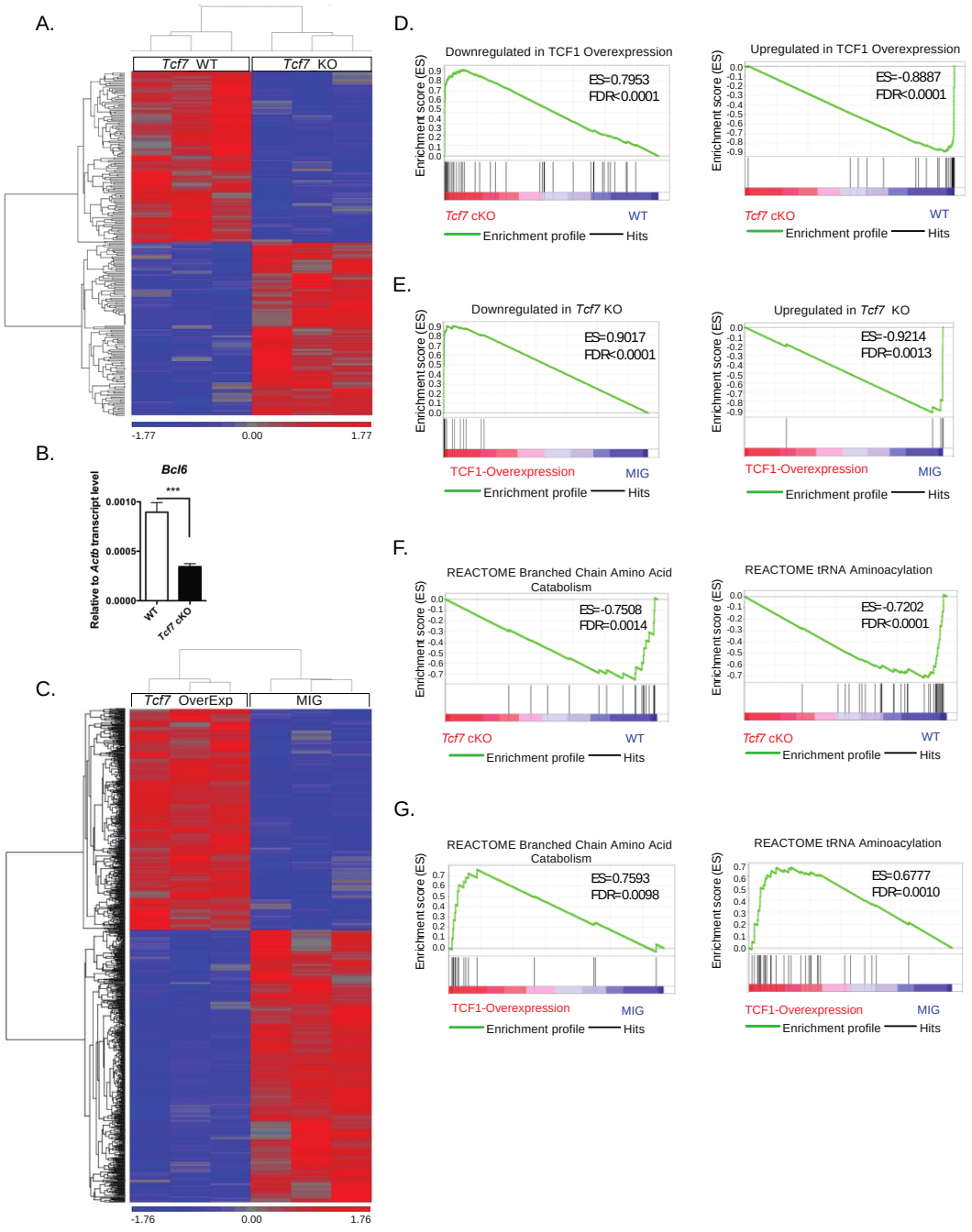

Fig. S6. GSEA of microarray data from TCF1 KO and overexpression experiments. The microarray experiments were described in Fig. 6. (A) Hierarchical clustering of microarray data in Table S2. (B) QRT-PCR analysis of *Bcl6* transcript levels in WT and TCF1 cKO tetramer^{+} CD8 T cells on day

7 p.i. *Actb* transcript levels were used as internal controls. Statistical significance was determined by unpaired t test. (C) Hierarchical clustering of microarray data in Table S3. (D) GSEA of the microarray data in Fig. 6A to compare the enrichment of gene signatures down-regulated by TCF1 over-expression (left) or up-regulated by TCF1 over-expression (right) between WT and cKO virus-specific CD8 T cells. (E) GSEA of the microarray data in Fig. 6C to compare the enrichment of gene signatures down-regulated by TCF1 knockout (left) or up-regulated by TCF1 knockout (right) between MIG and TCF1 over-expression constructs transduced P14 T cells. (F, G) GSEA of microarray data that compared branched-chain amino acid catabolism and tRNA aminoacylation signatures between WT and cKO virus-specific CD8 T cells (F) and between MIG and TCF1 over-expression constructs transduced P14 T cells (G).

Figure S7

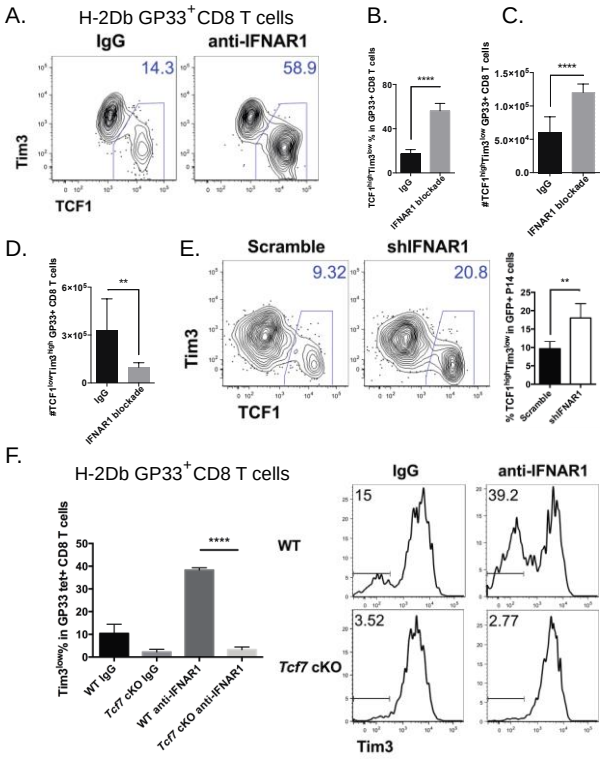

Fig. S7. Type I IFN blockade enhanced the generation of TCF1^{high}Tim3^{low} virus-specific CD8 T cells. (A-D) C57Bl6 mice were treated with 1mg of anti-IFNAR or isotype control IgG prior to infection. Splenocytes were analyzed on day 7 p.i. (A) Representative FACS plots of TCF1 and Tim3 expression in H-2Db GP33 tetramer$^+$ CD8 T cells from each group. Frequencies (B) and numbers (C) of TCF1^{high}Tim3^{low} GP33 tetramer$^+$ CD8 T cells in each group. (D) Numbers of TCF1^{low}Tim3^{high} GP33 tetramer$^+$ CD8 T cells in each group. (**E**) P14 cells transduced with retroviral constructs with IFNAR1 knockdown sequence or scrambled sequence were transferred into NK-cell depleted C57Bl6 mice that were infected with LCMV clone 13 after transfer. The differentiation of TCF1^{high}Tim3^{low} cells within transduced (GFP$^+$) P14 cells were analyzed on day 8 p.i. (F) WT and *Tcf7* cKO mice were treated with 1mg of anti-IFNAR or isotype control IgG prior to infection. Splenocytes were analyzed on day 7 p.i. Representative histograms of Tim3 expression in GP33 tetramer$^+$ CD8 T cells and frequencies of

Tim3^{low} cells within GP33 tetramer^{+} CD8 T cells in each group were shown. Data are representative of two independent experiments with n≥3. Statistical significance was determined by unpaired t tests.

Table S1. Differentially expressed genes between Tim3^{-}Blimp1^{-} and Tim3^{+}Blimp1^{+} CD8 T cells.

Table S2. Differentially expressed genes between Tcf7 KO and WT CD8 T cells.

Table S3. Differentially expressed genes between TCF1-overexpressing and MIG P14 cells.

Table S4. Raw data and statistical analyses.